Inhibition of soluble epoxide hydrolase modulates inflammation and autophagy in obese adipose tissue and liver: Role for omega-3 epoxides

Cristina López-Vicario[a], José Alcaraz-Quiles[a], Verónica García-Alonso[a], Bibiana Rius[a], Sung H. Hwang[b], Esther Titos[a,c], Aritz Lopategi[a], Bruce D. Hammock[b,1], Vicente Arroyo[c,d], and Joan Clària[a,c,e,1]

[a]Department of Biochemistry and Molecular Genetics, [d]Liver Unit, Hospital Clínic, Institut d'Investigacions Biomèdiques August Pi i Sunyer (IDIBAPS), [c]Centro de Investigación Biomédica en Red Enfermedades Hepáticas y Digestivas, and [e]Department of Physiological Sciences I, University of Barcelona, Barcelona 08036, Spain; and [b]Department of Entomology and Comprehensive Cancer Center, University of California, Davis, CA 95616

Contributed by Bruce D. Hammock, December 4, 2014 (sent for review July 25, 2014; reviewed by Karsten Gronert and Steve Watkins)

Soluble epoxide hydrolase (sEH) is an emerging therapeutic target in a number of diseases that have inflammation as a common underlying cause. sEH limits tissue levels of cytochrome P450 (CYP) epoxides derived from omega-6 and omega-3 polyunsaturated fatty acids (PUFA) by converting these antiinflammatory mediators into their less active diols. Here, we explored the metabolic effects of a sEH inhibitor (*t*-TUCB) in *fat-1* mice with transgenic expression of an omega-3 desaturase capable of enriching tissues with endogenous omega-3 PUFA. These mice exhibited increased CYP1A1, CYP2E1, and CYP2U1 expression and abundant levels of the omega-3–derived epoxides 17,18-epoxyeicosatetraenoic acid (17,18-EEQ) and 19,20-epoxydocosapentaenoic (19,20-EDP) in insulin-sensitive tissues, especially liver, as determined by LC-ESI-MS/MS. In obese *fat-1* mice, *t*-TUCB raised hepatic 17,18-EEQ and 19,20-EDP levels and reinforced the omega-3–dependent reduction observed in tissue inflammation and lipid peroxidation. *t*-TUCB also produced a more intense antisteatotic action in obese *fat-1* mice, as revealed by magnetic resonance spectroscopy. Notably, *t*-TUCB skewed macrophage polarization toward an antiinflammatory M2 phenotype and expanded the interscapular brown adipose tissue volume. Moreover, *t*-TUCB restored hepatic levels of Atg12-Atg5 and LC3-II conjugates and reduced p62 expression, indicating up-regulation of hepatic autophagy. *t*-TUCB consistently reduced endoplasmic reticulum stress demonstrated by the attenuation of IRE-1α and eIF2α phosphorylation. These actions were recapitulated in vitro in palmitate-primed hepatocytes and adipocytes incubated with 19,20-EDP or 17,18-EEQ. Relatively similar but less pronounced actions were observed with the omega-6 epoxide, 14,15-EET, and nonoxidized DHA. Together, these findings identify omega-3 epoxides as important regulators of inflammation and autophagy in insulin-sensitive tissues and postulate sEH as a druggable target in metabolic diseases.

obesity | inflammation | autophagy | omega-3–derived epoxides | soluble epoxide hydrolase

Cytochrome P450 (CYP) epoxygenases represent the third branch of polyunsaturated fatty acid (PUFA) metabolism (1). CYP epoxygenases add oxygen across one of the four double bonds of PUFA to generate three-membered ethers known as epoxides (1). In the case of arachidonic acid, CYP epoxygenases convert this omega-6 PUFA into epoxyeicosatrienoic acids (EETs), which act as autocrine or paracrine factors in the regulation of vascular tone, inflammation, hyperalgesia, and organ and tissue regeneration (2, 3). In addition to omega-6s, CYP epoxygenases also convert the omega-3 PUFA eicosapentaenoic acid (EPA) and docosahexaenoic acid (DHA) into novel epoxyeicosatetraenoic (EEQs) and epoxydocosapentaenoic (EDPs) acids, respectively (4, 5). These omega-3–derived epoxides also exert salutary actions and are even more effective and potent than omega-6–derived EETs (4–8).

Because the predicted in vivo half-lives of fatty acid epoxides (EpFA) are in the order of seconds (9), drugs that stabilize their levels by targeting the enzyme soluble epoxide hydrolase (sEH) are currently under investigation. sEH is a cytosolic enzyme with epoxide hydrolase and lipid phosphatase activities that catalyzes the rapid hydrolysis of EETs, EEQs and EDPs by adding water to these EpFA and converting them into inactive or less active 1,2-diols (10). Accordingly, inhibition of sEH exerts beneficial actions in controlling vascular tone, inflammation, and pain, and this strategy has shown its therapeutic potential for long-term use in hypertension, diabetes, renal disease, organ damage, and vascular remodeling (6, 9–12).

The aim of the present study was to investigate the potential metabolic benefits of sEH inhibition in obesity. Specifically, this study addresses the question as to whether sEH inhibition increases the effectiveness of omega-3–derived epoxides in obese adipose tissue and liver in the context of enriched omega-3 tissue content. *fat-1* mice with transgenic expression of the *Caenorhabditis elegans* omega-3 fatty acid desaturase gene represent a useful model to address this question because these mice have abundant tissue omega-3 distribution from their embryonic stage

Significance

Our study demonstrates that stabilization of cytochrome P-450 epoxides derived from omega-3 polyunsaturated fatty acids through inhibition of the inactivating enzyme soluble epoxide hydrolase (sEH) exerts beneficial actions in counteracting metabolic disorders associated with obesity. In addition, our study sheds more light on the role of sEH in cellular homeostasis by providing evidence that omega-3 epoxides and sEH inhibition regulate autophagy and endoplasmic reticulum stress in insulin-sensitive tissues, especially the liver. Therefore, administration of a sEH inhibitor is a promising strategy to prevent obesity-related comorbidities.

Author contributions: C.L.-V., V.A., and J.C. designed research; C.L.-V., J.A.-Q., V.G.-A., B.R., E.T., A.L., and J.C. performed research; C.L.-V., S.H.H., and B.D.H. contributed new reagents/analytic tools; C.L.-V. and J.C. analyzed data; and C.L.-V., B.D.H., and J.C. wrote the paper.

Reviewers: K.G., University of California, Berkeley; and S.W., Lipomics Technologies Inc.

Conflict of interest statement: B.D.H. and S.H.H. are authors on a patent held by the University of California on the synthesis of soluble epoxide hydrolase (sEH) inhibitors. B.D.H. founded a company, EicOsis, to move these inhibitors to the clinic to treat neuropathic and inflammatory pain. The published and freely available sEH inhibitor was provided by University of California, Davis to the Claria group in Spain along with additional reagents and data. The inhibitor was a key tool to test the hypothesis that the omega-6 and 3 fatty acid epoxides were responsible for biological effects. It is conceivable that use of an sEH inhibitor could be of some benefit to EicOsis or GSK, both of which are working to develop these materials clinically. However, numerous papers have been published already implicating these inhibitors in diabetes treatment, and other inhibitors of similar structure and potency are commercially available from Cayman Chemical and CalBiochem. B.D.H. is an author on University of California patents in the area, has stock in EicOsis, which has licensed these patents, but has no salary from EicOsis.

[1]To whom correspondence may be addressed. Email: jclaria@clinic.ub.es or bdhammock@ucdavis.edu.

This article contains supporting information online at www.pnas.org/lookup/suppl/doi:10.1073/pnas.1422590112/-/DCSupplemental.

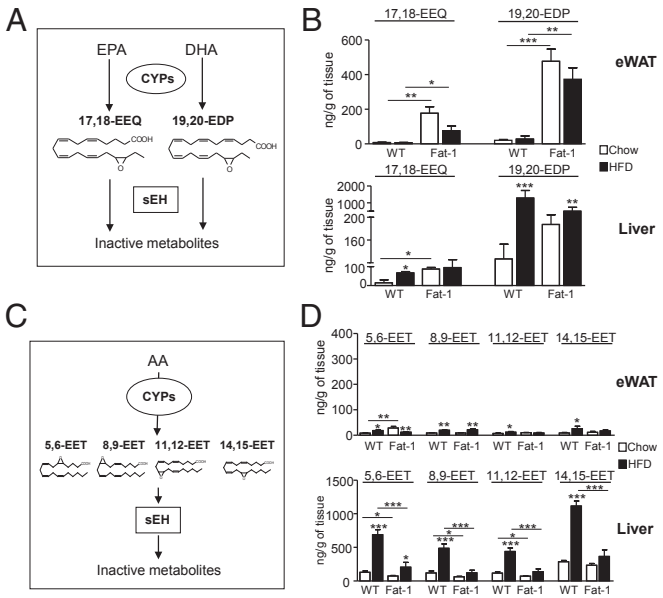

Fig. 1. Tissue levels of omega-3–derived epoxy metabolites, 17,18-EEQ and 19,20-EDP, in *fat-1* mice. (*A*) Schematic diagram of the CYP epoxygenation pathway generating the omega-3 EpFA, 17,18-EEQ, and 19,20-EDP and conversion into their inactive diols by sEH. (*B*) LC-ESI-MS/MS analysis of 17,18-EEQ and 19,20-EDP levels in eWAT and liver from WT and *fat-1* mice. (*C*) Schematic diagram of the CYP epoxygenation pathway generating omega-6 EpFA (5,6-EET, 8,9-EET, 11,12-EET, and 14,15-EET) from arachidonic acid (AA) and their inactivation by sEH. (*D*) LC-ESI-MS/MS analysis of omega-6 EpFA levels in eWAT and liver. Results are mean ± SEM from WT ($n = 28$) and *fat-1* ($n = 20$) mice. $^*P < 0.05$, $^{**}P < 0.01$, and $^{***}P < 0.001$.

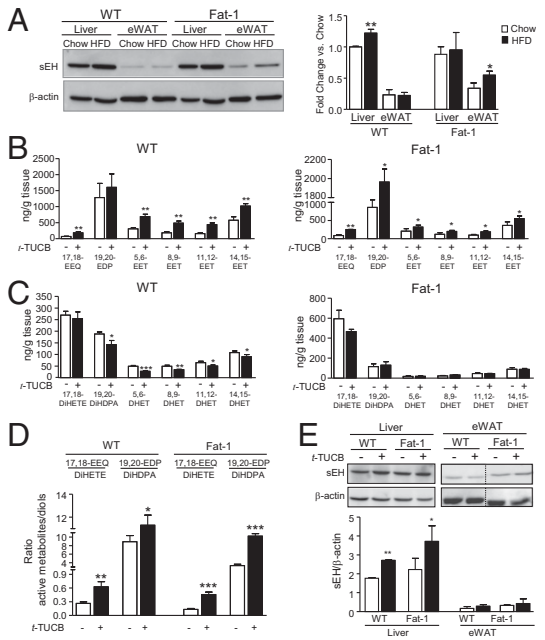

Fig. 2. sEH overexpression and modulation of 17,18-EEQ and 19,20-EDP tissue levels by the selective sEH inhibitor, *t*-TUCB. (*A*) Protein expression of sEH in liver and eWAT from WT and *fat-1* mice. Densitometry of sEH signals normalized to β-actin is shown on the right. (*B*) LC-ESI-MS/MS analysis of omega-3 and omega-6 epoxides in liver from HFD-induced obese WT and *fat-1* mice receiving *t*-TUCB (10 μg/mL) for 16 wk. (*C*) LC-ESI-MS/MS analysis of inactive diols in livers from obese WT and *fat-1* mice receiving *t*-TUCB. (*D*) Hepatic ratios of active metabolites to inactive diols. (*E*) Protein expression of sEH in liver and eWAT from obese WT and *fat-1* mice receiving *t*-TUCB. Densitometry of sEH signals normalized to β-actin is shown below. Results are mean ± SEM from WT ($n = 28$) and *fat-1* ($n = 20$) mice. $^*P < 0.05$, $^{**}P < 0.01$, and $^{***}P < 0.001$.

and throughout their lives (13, 14). This study builds on previous work by our laboratory demonstrating that *fat-1* mice replicate the protection against insulin resistance and hepatic inflammation and steatosis observed in obese mice nutritionally enriched with exogenous omega-3 PUFA (13, 15). The results of the present investigation indicate that inhibition of sEH when there is an increased content of omega-3 PUFA exerts a more favorable role in counteracting the metabolic disorders associated with obesity. In addition, our findings expand focus to include EpFA to the protective actions described for those lipid mediators derived from omega-3s through lipoxygenase- and cycloxygenase-initiated pathways (i.e., resolvins, protectins, and maresins) (16, 17).

Results

WT and *fat-1* mice had similar body and epididymal white adipose tissue (eWAT) weights under Chow conditions (Fig. S1*A*). However, *fat-1* mice exhibited smaller adipocyte size (Fig. S1*B*). The administration of a high-fat diet (HFD) resulted in increased adipocyte hypertrophy and extensive positive F4/80 staining (Fig. S1*B*). HFD-fed mice also displayed enhanced fibrosis (Fig. S1*B*). Compared with WT, *fat-1* mice were more resistant to HFD-induced obesity (body weight: 45.6 ± 0.8 vs. 49.7 ± 1.0 g, $P < 0.01$; eWAT weight: 1.5 ± 0.1 vs. 1.8 ± 0.1 g, $P < 0.01$) and showed reduced adipocyte size, macrophage infiltrate, and fibrosis (Fig. S1*B*). Changes in adiposity, inflammation and fibrosis were confirmed by morphometric analysis and by assessing F4/80 expression by real-time PCR (Fig. S1*B*). *fat-1* mice also showed reduced monocyte chemoattractant protein 1 (MCP-1) and increased CD206, IL-10, and macrophage galactose-type C-type lectin 1 (MGL1) (Fig. S1*C*). These results were confirmed in HFD-induced obese mice receiving omega-3 PUFA through the diet (Fig. S1*D*). No changes in IL-6, IL-1β, arginase-1 (Arg1), resistin-like molecule-α (RELMα), and Ym1 were observed (Fig. S1*D*). eWAT from both lean WT and *fat-1* mice had constitutive expression of CYP epoxygenases with preference for omega-3 PUFA (Fig. S1*E*). In response to the HFD, CYP expression was repressed in WT mice, whereas CYP1A1

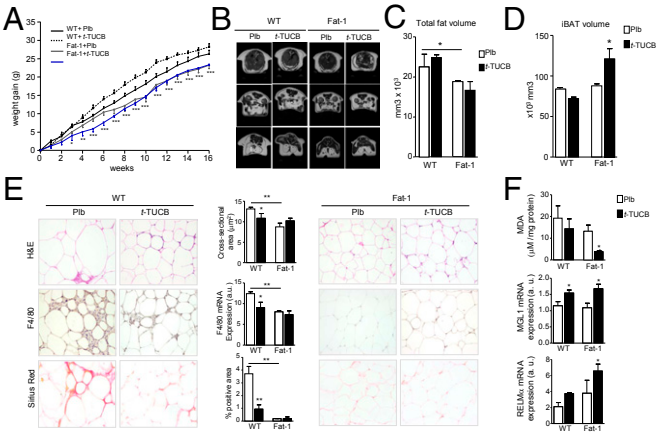

Fig. 3. Effects of *t*-TUCB on adipose tissue in obese *fat-1* mice. (*A*) Body weight curves for WT ($n = 28$) and *fat-1* ($n = 20$) mice receiving a HFD and treated with either placebo (Plb) or *t*-TUCB for 16 wk. (*B*) Representative MR images of coronal sections. Total fat volume (*C*) and iBAT volume (*D*) assessed by MRI analysis. (*E*) Representative photomicrographs of adipose tissue sections stained with H&E (*Top*), F4/80 (*Middle*), and Sirius red (*Bottom*) and adipocyte cross-sectional area, Sirius red staining, and F4/80 mRNA expression. (Magnification: 200×.) (*F*) Malondialdehyde (MDA) concentration and MGL1 and RELMα mRNA expression in adipose tissue. Results are mean ± SEM $^*P < 0.05$, $^{**}P < 0.01$, and $^{***}P < 0.001$.

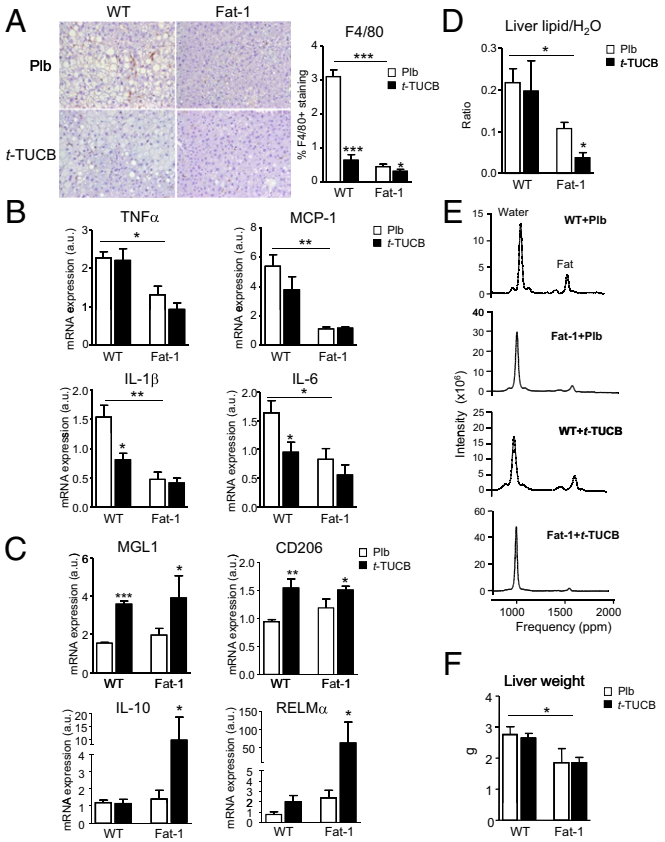

Fig. 4. Antiinflammatory and antisteatotic actions of *t*-TUCB in livers from obese *fat-1* mice. (*A*) Representative photomicrographs of liver sections stained with F4/80 and histomorphometrical analysis in HFD-induced obese WT and *fat-1* mice receiving placebo (Plb) or *t*-TUCB (10 μg/mL) for 16 wk. (Magnification: 200×.) (*B*) Hepatic mRNA expression of M1 proinflammatory markers. (*C*) Hepatic mRNA expression of M2 antiinflammatory markers. (*D*) Hepatic steatosis assessed by MR spectroscopy. (*E*) Representative spectra. (*F*) Liver weight. Results are mean ± SEM from WT ($n = 28$) and *fat-1* ($n = 20$) mice. $^{*}P < 0.05$, $^{**}P < 0.01$, and $^{***}P < 0.001$.

was induced in *fat-1* mice with no changes in CYP2E1 and CYP2U1 (Fig. S1*E*).

Because—in addition to adipose tissue—the liver plays a pivotal role in metabolic homeostasis, we also examined the hepatic phenotype of *fat-1* mice. Consistent with our recent finding that *fat-1* mice are protected against HFD-induced hepatic inflammation and steatosis (13), HFD-fed *fat-1* mice presented lower serum ALT/AST and reduced F4/80 and Oil Red-O staining (Fig. S2*A*). Moreover, HFD-fed WT mice exhibited a unique hepatic pattern of CYP expression characterized by up-regulation of CYP1A1, CYP2E1, and CYP2U1 (Fig. S2*B*). In contrast, only CYP2U1 was up-regulated by HFD feeding in *fat-1* mice (Fig. S2*B*). A distinct pattern of CYP expression in response to HFD was also detected in skeletal muscle (Fig. S2*C*). Direct comparison of CYP expression among insulin-sensitive tissues revealed that CYP2E1 and CYP2U1 are preferentially expressed in the liver, whereas CYP1A1 appears as the major isoform in muscle (Fig. S2*D*). The observation that changes in CYP expression in HFD-fed mice in response to omega-3 enrichment are tissue-dependent was confirmed in obese WT mice receiving omega-3 PUFA through the diet (Fig. S3).

Because many CYP epoxygenases can form epoxides converting omega-3 PUFA into biologically active 17,18-EEQ and 19,20-EDP metabolites (Fig. 1*A*), we next analyzed these epoxides by liquid chromatography-electrospray ionization (LC-ESI)-MS/MS. Both EPA-derived 17,18-EEQ and DHA-derived 19,20-EDP were detected in eWAT and liver (Fig. 1*B*). Importantly, 17,18-EEQ levels were significantly increased in eWAT and liver from *fat-1* mice (Fig. 1*B*). In these tissues, 19,20-EDP was also increased in *fat-1* mice and changes in this epoxide reached statistical significance in eWAT (Fig. 1*B*). Unexpectedly, HFD triggered omega-3–derived epoxides in the liver, especially in WT mice (Fig. 1*B*). Increased tissue levels of omega-3–derived epoxides were also seen in eWAT and liver from obese WT mice after receiving an omega-3–enriched diet (Fig. S4*A*). On the other hand, EETs regioisomers (5,6-EET, 8,9-EET, 11,12-EET, and 14,15-EET), formed from arachidonic acid by CYP epoxidation (Fig. 1*C*), were also detected in eWAT and especially in liver (Fig. 1*D*). Hepatic EET levels were also increased by HFD (Fig. 1*D*), an effect also seen in WT mice receiving an omega-3–enriched diet (Fig. S4*B*). The fact that omega-3– and omega-6–derived epoxides were more abundant in liver (Fig. 1 *B* and *D*) was consistent with the presence of a higher content of PUFA in this organ (Fig. S5*A*). Moreover, although the rate-limiting enzymes involved in long-chain fatty acid desaturation (i.e., Δ5 and Δ6 desaturases) were constitutively expressed in liver, the expression of Δ6 desaturase in eWAT was undetectable and residual at protein (Fig. S5*B*) and mRNA (Fig. S5*C*) levels, respectively.

We next sought to establish the role of sEH, the key enzyme in the inactivation of EpFA. Consistent with previous findings, the sEH protein was preferentially expressed in liver (18) and slightly

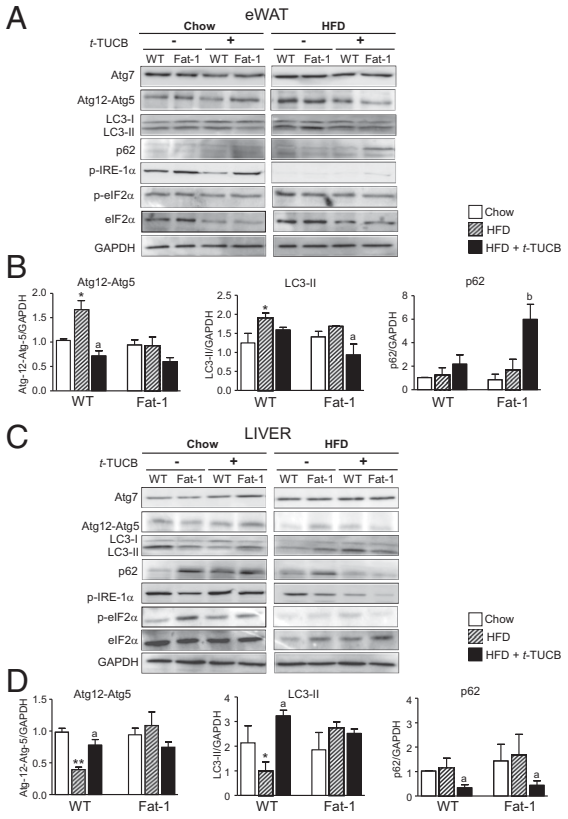

Fig. 5. *t*-TUCB regulates in a tissue-specific manner autophagy and ER stress in obese *fat-1* mice. (*A*) Protein expression of Atg7, Atg12-Atg5, LC3-I/II, p62, phosphoIRE-1α (p-IRE-1α), phosphoeIF2α (p-eIF2α), total eIF2α (eIF2α), and GAPDH as determined by 10% SDS/PAGE Western blot in eWAT from WT and *fat-1* mice receiving Chow or HFD and treated with *t*-TUCB (10 μg/mL) for 16 wk. (*B*) Densitometric analysis of Atg12-Atg5, LC3-I/II, and p62 signals normalized to GAPDH in eWAT. (*C*) Hepatic protein expression of Atg-7, Atg12-Atg5, LC3-I/II, p62, p-IRE-1α, p-eIF2α, eIF2α, and GAPDH. (*D*) Densitometric analysis of Atg12-Atg5, LC3-I/II, and p62 signals normalized to GAPDH in liver. Results are mean ± SEM from WT ($n = 28$) and *fat-1* ($n = 20$) mice. $^{*}P < 0.05$ and $^{**}P < 0.01$ vs. Chow. $^{a}P < 0.05$ and $^{b}P < 0.001$ vs. HFD.

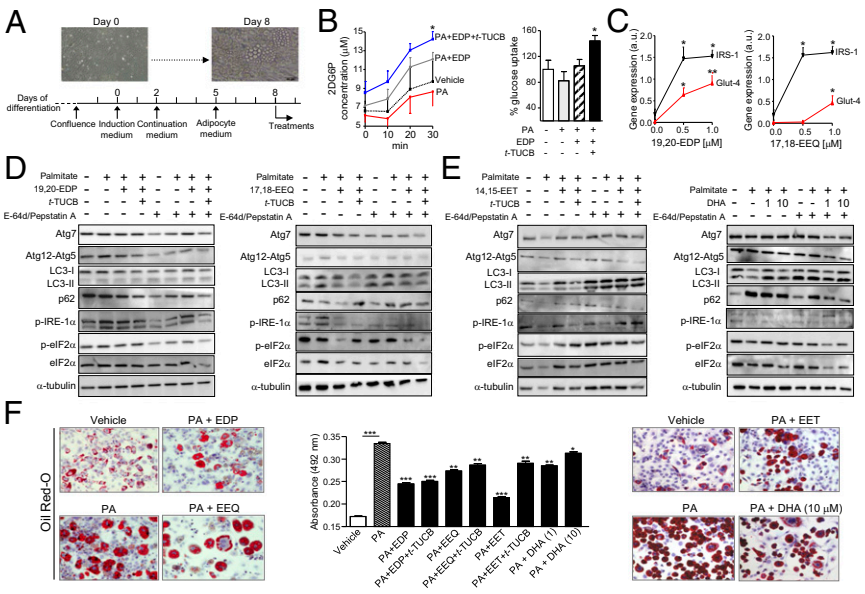

Fig. 6. In vitro effects of EpFA on glucose uptake, autophagy, ER stress, and lipid accumulation in differentiated 3T3-L1 adipocytes. (*A*) Scheme of the in vitro experiments. Visible microscope images at days 0 and 8 of differentiation are shown. (*B*, *Left*) Glucose uptake assessed by the 2-deoxyglucose assay in cells incubated with vehicle or sodium palmitate (PA) alone or in combination with 19,20-EDP (EDP) and *t*-TUCB for 30 min. (*Right*) Quantitation of endpoint glucose uptake. (*C*) GLUT-4 and IRS-1 expression in cells exposed to 19,20-EDP (*Left*) or 17,18-EEQ (*Right*) in the presence of PA. (*D* and *E*) Western blots (15% SDS/PAGE) of Atg7, Atg12-Atg5, LC3-I/II, p62, phosphoIRE-1α (p-IRE-1α), phosphoeIF2α (p-eIF2α), total eIF2α (eIF2α), and α-tubulin in cells incubated with vehicle or PA (0.5 mM) alone or in combination with *t*-TUCB (1 μM), 19,20-EDP (1 μM), 17,18-EEQ (1 μM), 14,15-EET (1 μM), and DHA (1 and 10 μM) in the absence or presence of the protease inhibitors E-64d/pepstatin A for 24 h. (*F*) Representative photomicrographs of Oil Red-O–stained cells incubated with the same conditions as *D* and *E*. (Magnification: 200×.) The amount of Oil Red-O retained is shown on the middle. Results are mean ± SEM from three independent experiments assayed in triplicate. $*P < 0.05$, $**P < 0.005$, and $***P < 0.001$.

increased by HFD feeding (Fig. 2*A*). In *fat-1* mice, HFD-feeding also increased sEH expression in eWAT (Fig. 2*A*). Because inhibition of the sEH prevents the inactivation of EpFA by epoxide hydration, we next analyzed the omega-3–derived epoxides in mice treated with the selective sEH inhibitor, *trans*-4-{4-[3-(4-trifluoromethoxy-phenyl)-ureido]-cyclohexyloxy}-benzoic acid (*t*-TUCB). Administration of *t*-TUCB to HFD-induced obese mice resulted in increased 17,18-EEQ levels in liver (Fig. 2*B*) and eWAT (Fig. S5*D*) from both WT and *fat-1* mice. Tissue levels of 19,20-EDP were increased in livers from *fat-1* mice and eWAT from WT animals (Fig. 2*B* and Fig. S5*D*). *t*-TUCB also increased levels of EETs in liver and eWAT from both WT and *fat-1* mice, although the extent of stimulation was less pronounced than that of 19,20-EDP (Fig. 2*B* and Fig. S5*D*). Hepatic levels of 19,20-DiHDPA, the inactive or less active 1,2-diol from 19,20-EDP, as well as the respective EETs diols were significantly reduced by *t*-TUCB in WT mice (Fig. 2*C*). No changes in diol levels were observed in *fat-1* mice (Fig. 2*C*). Of note, the hepatic ratios of each active epoxide to the corresponding inactive diol were significantly increased by *t*-TUCB (Fig. 2*D*). Compared with placebo, *t*-TUCB did not induce any significant effect on the hepatic and adipose tissue levels of arachidonic acid, DHA and EPA (Table S1). Coincident with previous findings (19), *t*-TUCB up-regulated hepatic sEH protein expression (Fig. 2*E*).

Because sEH inhibition is associated with salutary effects, we next assessed the metabolic actions of *t*-TUCB in mice with HFD-induced obesity. As shown in Fig. 3*A*, *t*-TUCB did not modify weight gain in WT mice or alter the resistance of *fat-1* mice to become obese. Consequently, endpoint body weight was only influenced by the *fat-1* phenotype (Fig. S6*A*). Anatomical 7.0T magnetic resonance (MR) imaging analysis confirmed reduced total fat volume in *fat-1* mice and absence of changes in this parameter following *t*-TUCB treatment (Fig. 3 *B* and *C* and Fig. S6*B*). Interestingly, interscapular brown adipose tissue (iBAT) volume was increased in *fat-1* mice treated with *t*-TUCB (Fig. 3*D* and Fig. S6*C*). Despite the absence of changes in total fat volume, *t*-TUCB significantly reduced adipocyte hypertrophy, macrophage infiltration, and adipose tissue fibrosis in obese WT mice (Fig. 3*E*). No further reduction in these adiposity parameters was observed in obese *fat-1* mice receiving *t*-TUCB (Fig. 3*E*). These findings were confirmed by morphometric analysis and the assessment of F4/80 mRNA expression (Fig. 3*E*). Changes in adipose tissue fibrosis were also confirmed by Masson's trichrome staining (Fig. S6*D*). Of interest, *t*-TUCB significantly reduced lipid peroxidation in *fat-1* mice and up-regulated the expression of MGL1 and RELMα in both WT and *fat-1* mice (Fig. 3*F*).

The effects of *t*-TUCB on the liver are shown in Fig. 4. *t*-TUCB effectively blocked HFD-induced hepatic macrophage infiltration in WT mice, an effect that was more intense in *fat-1* mice (Fig. 4*A*). Consistently, *t*-TUCB decreased hepatic IL-1β and IL-6 expression (Fig. 4*B*), while up-regulating MGL1 and CD206 (Fig. 4*C*). M2 polarization of hepatic macrophages was more evident in *fat-1* mice receiving *t*-TUCB (Fig. 4*C*). In addition to reducing inflammation, *t*-TUCB decreased the hepatic lipid content and induced a synergistic antisteatotic action in *fat-1* mice, as detected by MR spectroscopy (Fig. 4*D*). Representative spectra are depicted in Fig. 4*E*. The reduction of liver weight in *fat-1* mice was not further decreased by *t*-TUCB (Fig. 4*F*).

Because dysregulation of autophagy is a critical component of liver and eWAT dysfunction in obesity (20), we next investigated the effects of sEH inhibition on autophagy and the emergence of endoplasmic reticulum (ER) stress, insulin resistance, and lipid deposition in obesity. Consistent with previous studies (21, 22), HFD-induced obesity increased the activity of the molecular indicators of autophagy, Atg12-Atg5, and LC3-II, in eWAT from WT mice, effects that were reversed by *t*-TUCB treatment (Fig. 5 *A* and *B*). No changes in Atg12-Atg5 and LC3-II conjugates were observed in *fat-1* mice after HFD feeding, but LC3-II was reduced and p62 was increased by *t*-TUCB (Fig. 5 *A* and *B*). On the other hand, in livers from WT mice, HFD-induced obesity was associated with reduced Atg12-Atg5 and LC3-II levels, and these markers of autophagy were restored by *t*-TUCB (Fig. 5 *C* and *D*). Reduced autophagy was not observed in livers from *fat-1* mice, suggesting that these mice were already protected from HFD-induced autophagy dysfunction (Fig. 5 *C* and *D*). Taken together, and considering that Atg12-Atg5 and LC3-II conjugates are required for autophagosome formation and that the induction of p62 levels indicates a lack of functional autophagic degradation (23), our data suggest that sEH inhibition improves the autophagy flux in obese insulin-sensitive tissues. Finally, consistent with the view that autophagy is integrated to ER homeostasis (20), *t*-TUCB administration resulted in reduced ER stress, as shown by the attenuation of inositol-requiring enzyme 1α (IRE-1α) and eukaryotic initiation factor 2 (eIF2α) phosphorylation in both eWAT and liver (Fig. 5 *A* and *C*). The extent of suppression of ER stress by *t*-TUCB was roughly similar in WT and *fat-1* mice (Fig. 5 *A* and *C*).

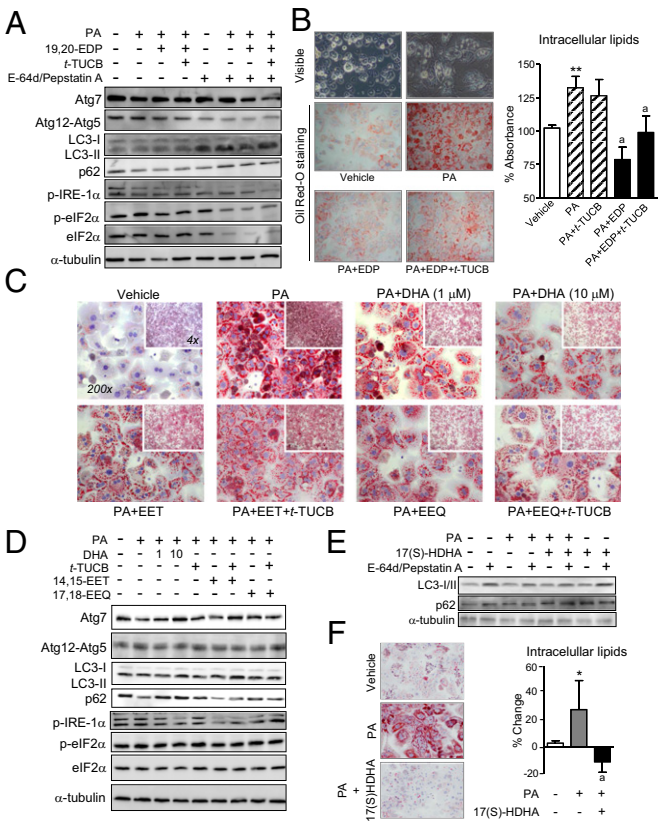

Fig. 7. In vitro effects of EpFA on autophagy, ER stress, and lipid accumulation in primary hepatocytes. (*A*) Western blots (15% SDS/PAGE) of Atg7, Atg12-Atg5, LC3-I/II, p62, phosphoIRE-1α (p-IRE-1α), phosphoeIF2α (p-eIF2α), total eIF2α (eIF2α), and α-tubulin in hepatocytes incubated with vehicle or palmitate (PA) (0.5 mM) in combination with 19,20-EDP (1 μM) and *t*-TUCB (1 μM) in the absence or presence of E-64d/pepstatin A for 24 h. (*B*) Representative photomicrographs of visible microscope (*Top*) and Oil Red-O–stained (*Middle* and *Bottom*) hepatocytes exposed to vehicle or PA alone or in combination with 19,20-EDP (EDP) and *t*-TUCB for 24 h. The amount of Oil Red-O retained is shown on the right. (*C*) Representative photomicrographs of Oil Red-O–stained hepatocytes exposed to either vehicle or PA alone or in combination with 17,18-EEQ (EEQ, 1 μM), 14,15-EET (EET, 1 μM), DHA (1 and 10 μM), and *t*-TUCB (1 μM) for 24 h. (*D*) Western blot analysis of Atg7, Atg12-Atg5, LC3-I/II, p62, p-IRE-1α, p-eIF2α, eIF2α, and α-tubulin in hepatocytes incubated with the same conditions as in *C*. (*E*) Protein expression of LC3-I/II, p62 and α-tubulin in hepatocytes incubated with vehicle or PA in combination with 17(S)-HDHA (1 μM). (*F*) Amount of Oil Red-O retained by hepatocytes in response to PA and 17(S)-HDHA. Results are mean ± SEM from four independent experiments assayed in triplicate. $*P < 0.01$ and $**P < 0.001$ vs. vehicle. a, $P < 0.05$ vs. PA. (Magnification: 200×.)

To provide direct evidence linking omega-3 EpFA to autophagy and ER stress, we next performed in vitro experiments in adipocytes incubated with the saturated fatty acid palmitate, a major contributor to lipotoxicity and insulin resistance (24). A schematic diagram of the experimental in vitro procedure is shown in Fig. 6*A*. Incubation of adipocytes with 19,20-EDP, the most abundant omega-3 epoxide in eWAT, in the presence of *t*-TUCB, stimulated glucose uptake in adipocytes (Fig. 6*B*). Moreover, in these cells, 19,20-EDP and 17,18-EEQ induced a concentration-dependent up-regulation of insulin receptor substrate-1 (IRS-1) and glucose transporter-type 4 (GLUT-4) (Fig. 6*C*). Interestingly, in the presence of *t*-TUCB, both 19,20-EDP and 17,18-EEQ produced similar changes in autophagy to those reported in vivo in eWAT from obese *fat-1* mice receiving *t*-TUCB (Fig. 6*D*). With *t*-TUCB on board, reduction of IRE-1α and eIF2α phosphorylation in response to these omega-3 EpFA also paralleled that seen in vivo (Fig. 6*D*). In these experiments, the omega-6 EpFA, 14,15-EET, and the nonoxidized form of DHA were either ineffective or less active than omega-3 EpFA in regulating authophagy and ER stress in adipocytes (Fig. 6*E*). All compounds tested significantly reduced palmitate-induced accumulation of lipids in adipocytes, with the EpFA being more potent than the nonoxidized form of DHA (Fig. 6*F*). *t*-TUCB alone did not modify ER stress, autophagy, and intracellular lipid levels (Fig. S6*E*).

Finally, we incubated hepatocytes with palmitate in the presence of EpFA and *t*-TUCB. As shown in Fig. 7*A*, incubation of hepatocytes with 19,20-EDP and *t*-TUCB resulted in increased autophagosome formation, as revealed by the disappearance of LC3-I and its conversion to LC3-II by conjugation to phosphatidylethanolamine. This improvement in autophagy was mirrored by a reduction in the phosphorylated forms of IRE-1α and eIF2α, indicative of attenuated ER stress in hepatocytes (Fig. 7*A*). In these cells, 19,20-EDP also overrode palmitate-induced accumulation of intracellular lipids (Fig. 7*B*). Similar actions on intracellular lipid levels were observed with 17,18-EEQ as well as with DHA and 14,15-EET, although this omega-6 EpFA was less potent than the omega-3 epoxides (Fig. 7*C*). However, compared with 19,20-EDP, 17,18-EEQ, DHA, and 14,15-EET were less active in regulating autophagy and unable to modulate ER stress in hepatocytes (Fig. 7*D*). Finally, we explored the effects of 17 (S)-HDHA, a lipid mediator acting as a precursor and marker of the biosynthesis of the D-series resolvins and protectins derived from DHA through the lipoxygenase pathway (16). This hydroxylated DHA-derived product also enhanced autophagy in palmitate-treated hepatocytes (Fig. 7*E*), and reduced the accumulation of intracellular lipids in palmitate-primed hepatocytes (Fig. 7*F*). *t*-TUCB alone did not induce any change in the response of hepatocytes to palmitate (Fig. 7 *B* and *D*).

Discussion

Special attention has been given to the effects of omega-3 PUFA on the chronic "low-grade" inflammatory state driven by the expansion of adipose tissue mass in obesity (15, 25). This persistent inflammation in adipose tissue of obese individuals is deleterious and increases the incidence of comorbidities, including insulin resistance and nonalcoholic fatty liver disease, a condition in which a recent systematic meta-analysis reported the benefits of omega-3 PUFA therapy (26). In addition, our understanding the recognized therapeutic values of omega-3s has been challenged by the discovery that these fatty acids can be converted to a novel class of proresolving lipid mediators (i.e., resolvins, protectins, and maresins) (reviewed in ref. 16). Indeed, these proresolving mediators are able to counteract inflammation and to prime the resolution process in obesity-induced nonalcoholic fatty liver disease (17). A common feature of these proresolving lipid mediators is that their biosynthesis from omega-3 PUFA is initiated through the interaction of lipoxygenase and cyclooxygenase pathways, the two classic branches of PUFA metabolism (16). Recent findings indicate that CYP epoxygenases, the so-called third branch of PUFA metabolism, can also convert omega-3 PUFA into bioactive lipid mediators (1, 4, 5). Indeed, CYP1A1, CYP2E1, and CYP2U1 have been described to generate a number of CYP-derived epoxides (namely EEQs and EDPs) from omega-3 PUFA (4). In our study, we used *fat-1* mice as an optimal model of omega-3 enrichment, in which the stabilization of CYP-derived epoxides by a sEH inhibitor reinforced the omega-3–dependent reduction in hepatic inflammation and intrahepatic lipid deposition. Taken together, our findings expand to the metabolic field the initial observation that an omega-3–rich diet in combination with a sEH inhibitor exerts antihypertensive actions (6).

A salient feature of our study was that the sEH inhibitor restored autophagy in livers from obese *fat-1* mice. Defective autophagy contributes to a variety of diseases, because efficient sequestration and clearance of damaged cellular components in stress conditions is crucial for cell homeostasis (27). Moreover, consistent with the view that autophagy is a primordial cellular

adaptive mechanism that mitigates ER-associated unfavorable conditions in insulin-sensitive tissues (20), sEH inhibition in *fat-1* mice was accompanied by an attenuated hepatic ER stress. Down-regulation of ER stress was also seen in conjunction with decreased autophagy in adipose tissue from *fat-1* mice receiving the sEH inhibitor, suggesting dissociation between these two cellular processes in this tissue. Because inhibition of autophagic function in adipose tissue is related to reduced fat mass and improved insulin sensitivity (28), our findings in adipose tissue can be regarded as beneficial in terms of lipid homeostasis and metabolic control. A strong asset of our study was that we were able to recapitulate the effects on autophagy and ER stress seen in vivo following sEH inhibition, by exposing hepatocytes and adipocytes in vitro to the omega-3 epoxides 19,20-EDP and 17,18-EEQ. Our findings are consistent with those reported by Bettaieb et al., who showed attenuation of ER stress in adipose and liver tissues in mice either receiving a sEH inhibitor or deficient for sEH (29). However, our data cannot exclude other EpFA, such as the case of arachidonic acid-derived EETs as well as the potential implication of other oxidized lipid mediators derived from omega-3 PUFA through the interaction of lipoxygenase and cyclooxygenase pathway. Additionally, our data cannot exclude the potential implication of nonoxidized DHA in the observed favorable metabolic phenotype of *fat-1* mice. In this regard, although less potent than EpFA, DHA was active in our cell bioassays. This finding is consistent with the reported biological properties of DHA (30) and with findings reported by Caviglia et al. showing that DHA was able to rescue rat hepatoma cells from palmitate-induced ER stress (31). However, these studies did not address whether the protective effects of DHA were mediated by the parent nonoxidized molecule or by any other DHA oxidized metabolite (30, 31).

In summary, the results of the present study demonstrate that stabilization of omega-3 epoxides through inhibition of sEH exerts beneficial actions in counteracting the metabolic disorders associated with obesity. Of particular interest are the findings demonstrating the ability of sEH inhibition to restore autophagy in the liver with the consequent reduction of obesity-induced liver ER stress. Our observations highlight the potentiality of small bioactive lipid mediators to modulate autophagy, serving as templates for the exploitation of this housekeeping cellular process for therapeutic interventions against obesity and obesity-related comorbidities, such as fatty liver disease.

Materials and Methods

Studies in *fat-1* mice, hepatocytes and 3T3-L1 adipocytes, measurement of 2-deoxyglucose uptake, mRNA and protein expression, and histology and immunohistochemistry analysis, MR imaging and spectroscopy, and LC-ESI-MS/MS and gas chromatography analysis are described in detail in *SI Materials and Methods*. The LC-MS/MS conditions used to profile the omega-3 and omega-6 epoxides are described in Table S2 and a schematic diagram of the experimental design of the study can be found in Fig. S7.

ACKNOWLEDGMENTS. We thank Dr. J. X. Kang (Massachusetts General Hospital) for kindly providing *fat-1* mice, Dr. M. Cofan for gas chromatography analysis, and Anabel Martínez-Puchol for assistance. This work was conducted at the Centre Esther Koplowitz and was supported by Spanish Ministerio de Economía y Competitividad (MEC) (SAF12/32789 and PIE14/00045); the Research Investments in the Sciences and Engineering Program of the University of California, Davis; Grants R01 ES002710 and P42 ES004699 from the National Institute of Environmental Health Sciences; fellowships from MEC (to V.G.-A. and B.R.); Marie Curie Action (A.L.); and an Emili Letang fellowship (to J.A.-Q.). Centro de Investigación Biomédica en Red Enfermedades Hepáticas y Digestivas is funded by the Instituto de Salud Carlos III. C.L.-V. was supported by the Institut d'Investigacions Biomèdiques August Pi i Sunyer/Fundació Clínic.

1. Spector AA, Norris AW (2007) Action of epoxyeicosatrienoic acids on cellular function. *Am J Physiol Cell Physiol* 292(3):C996–C1012.
2. Zeldin DC (2001) Epoxygenase pathways of arachidonic acid metabolism. *J Biol Chem* 276(39):36059–36062.
3. Panigrahy D, et al. (2013) Epoxyeicosanoids promote organ and tissue regeneration. *Proc Natl Acad Sci USA* 110(33):13528–13533.
4. Arnold C, et al. (2010) Arachidonic acid-metabolizing cytochrome P450 enzymes are targets of ω-3 fatty acids. *J Biol Chem* 285(43):32720–32733.
5. Zhang G, et al. (2013) Epoxy metabolites of docosahexaenoic acid (DHA) inhibit angiogenesis, tumor growth, and metastasis. *Proc Natl Acad Sci USA* 110(16):6530–6535.
6. Ulu A, et al. (2014) An omega-3 epoxide of docosahexaenoic acid lowers blood pressure in angiotensin-II-dependent hypertension. *J Cardiovasc Pharmacol* 64(1):87–99.
7. Morisseau C, et al. (2010) Naturally occurring monoepoxides of eicosapentaenoic acid and docosahexaenoic acid are bioactive antihyperalgesic lipids. *J Lipid Res* 51(12):3481–3490.
8. Falck JR, et al. (2011) 17(R),18(S)-epoxyeicosatetraenoic acid, a potent eicosapentaenoic acid (EPA) derived regulator of cardiomyocyte contraction: structure-activity relationships and stable analogues. *J Med Chem* 54(12):4109–4118.
9. Shen HC (2010) Soluble epoxide hydrolase inhibitors: A patent review. *Expert Opin Ther Pat* 20(7):941–956.
10. Morisseau C, Hammock BD (2013) Impact of soluble epoxide hydrolase and epoxyeicosanoids on human health. *Annu Rev Pharmacol Toxicol* 53:37–58.
11. Schmelzer KR, et al. (2005) Soluble epoxide hydrolase is a therapeutic target for acute inflammation. *Proc Natl Acad Sci USA* 102(28):9772–9777.
12. Shaik JS, et al. (2013) Soluble epoxide hydrolase inhibitor trans-4-[4-(3-adamantan-1-yl-ureido)-cyclohexyloxy]-benzoic acid is neuroprotective in rat model of ischemic stroke. *Am J Physiol Heart Circ Physiol* 305(11):H1605–H1613.
13. López-Vicario C, et al. (2014) Molecular interplay between Δ5/Δ6 desaturases and long-chain fatty acids in the pathogenesis of non-alcoholic steatohepatitis. *Gut* 63(2):344–355.
14. Kang JX, Wang J, Wu L, Kang ZB (2004) Transgenic mice: *fat-1* mice convert n-6 to n-3 fatty acids. *Nature* 427(6974):504.
15. González-Périz A, et al. (2009) Obesity-induced insulin resistance and hepatic steatosis are alleviated by omega-3 fatty acids: A role for resolvins and protectins. *FASEB J* 23(6):1946–1957.
16. Serhan CN (2014) Pro-resolving lipid mediators are leads for resolution physiology. *Nature* 510(7503):92–101.
17. Rius B, et al. (2014) Resolvin D1 primes the resolution process initiated by calorie restriction in obesity-induced steatohepatitis. *FASEB J* 28(2):836–848.
18. De Taeye BM, et al. (2010) Expression and regulation of soluble epoxide hydrolase in adipose tissue. *Obesity (Silver Spring)* 18(3):489–498.
19. Liu Y, et al. (2012) Inhibition of soluble epoxide hydrolase attenuates high-fat-diet–induced hepatic steatosis by reduced systemic inflammatory status in mice. *PLoS ONE* 7(6):e39165.
20. Yang L, Li P, Fu S, Calay ES, Hotamisligil GS (2010) Defective hepatic autophagy in obesity promotes ER stress and causes insulin resistance. *Cell Metab* 11(6):467–478.
21. Nuñez CE, et al. (2013) Defective regulation of adipose tissue autophagy in obesity. *Int J Obes (Lond)* 37(11):1473–1480.
22. Jansen HJ, et al. (2012) Autophagy activity is up-regulated in adipose tissue of obese individuals and modulates proinflammatory cytokine expression. *Endocrinology* 153(12):5866–5874.
23. Klionsky DJ, et al. (2012) Guidelines for the use and interpretation of assays for monitoring autophagy. *Autophagy* 8(4):445–544.
24. Van Epps-Fung M, Williford J, Wells A, Hardy RW (1997) Fatty acid-induced insulin resistance in adipocytes. *Endocrinology* 138(10):4338–4345.
25. Buckley JD, Howe PRC (2009) Anti-obesity effects of long-chain omega-3 polyunsaturated fatty acids. *Obes Rev* 10(6):648–659.
26. Parker HM, et al. (2012) Omega-3 supplementation and non-alcoholic fatty liver disease: A systematic review and meta-analysis. *J Hepatol* 56(4):944–951.
27. Schneider JL, Cuervo AM (2014) Liver autophagy: Much more than just taking out the trash. *Nat Rev Gastroenterol Hepatol* 11(3):187–200.
28. Singh R, et al. (2009) Autophagy regulates adipose mass and differentiation in mice. *J Clin Invest* 119(11):3329–3339.
29. Bettaieb A, et al. (2013) Soluble epoxide hydrolase deficiency or inhibition attenuates diet-induced endoplasmic reticulum stress in liver and adipose tissue. *J Biol Chem* 288(20):14189–14199.
30. Oh DY, et al. (2010) GPR120 is an omega-3 fatty acid receptor mediating potent anti-inflammatory and insulin-sensitizing effects. *Cell* 142(5):687–698.
31. Caviglia JM, et al. (2011) Different fatty acids inhibit apoB100 secretion by different pathways: unique roles for ER stress, ceramide, and autophagy. *J Lipid Res* 52(9):1636–1651.